

Study on surface properties of UHMWPE/Hap composite coating on Ti6Al4V

Gözde Çelebi Efe & Elif Yenilmez

To cite this article: Gözde Çelebi Efe & Elif Yenilmez (2022) Study on surface properties of UHMWPE/Hap composite coating on Ti6Al4V, Surface Engineering, 38:4, 417-429, DOI: 10.1080/02670844.2022.2077558

To link to this article: <https://doi.org/10.1080/02670844.2022.2077558>



Published online: 29 May 2022.



Submit your article to this journal [↗](#)



Article views: 155



View related articles [↗](#)



View Crossmark data [↗](#)



Citing articles: 1 View citing articles [↗](#)



Study on surface properties of UHMWPE/Hap composite coating on Ti6Al4V

Gözde Çelebi Efe^a and Elif Yenilmez^b

^aFaculty of Technology, Metallurgical and Materials Engineering, Sakarya University of Applied Sciences, Sakarya, Turkey; ^bEngineering Faculty, Department of Metallurgy and Materials Engineering, Sakarya University, Sakarya, Turkey

ABSTRACT

In the present study, UHMWPE (Ultra High Molecular Weight Polyethylene)- 0.5, 1 and 2 wt-% Hap (hydroxyapatite) composite film coatings on Ti6Al4V alloy were produced by dip coating method. Homogeneous dispersion of Hap particles was detected by SEM (Scanning Electron Microscope) and FE-SEM (Field Emission Scanning Electron Microscope). The characteristic absorption peaks of Hap are observed by FTIR (Fourier Transform Infrared Spectroscopy). Hap addition caused the increment of the crystallinities of composites from 24.6% to 56.8% related with the increment of the melting temperatures. Composite coatings showed excellent wear resistance with the decreasing worn area of 96% and the friction coefficient of 97%, compared to the uncoated Ti6Al4V. The biocompatibility and wettability tests of all coated surfaces were performed. It is foreseen that UHMWPE/2wt-%Hap composite film coating on Ti6Al4V will be promising for Hip joint prosthesis.

ARTICLE HISTORY

Received 20 January 2022
Revised 15 April 2022
Accepted 10 May 2022

KEYWORDS

UHMWPE; hydroxyapatite; Ti6Al4V; dip-coating; prosthesis; wear; composite; crystallinity

Introduction

Biomaterials, which is a multidisciplinary field, are natural or artificial materials used to support the functions of living tissues that have lost their function in the human body [1]. An implant material must first be biocompatible, sufficiently durable, corrosion resistant, nontoxic, antiallergic and doesn't have any mutagenic or carcinogenic effects, and has an acceptable price/benefit ratio [2–4]. Pure titanium and its alloys are the most preferred material for biomedical applications due to their bone-near elastic modulus (120 GPa), durability, excellent corrosion resistance, load-bearing ability, lightness, non-toxicity and most importantly biocompatibility [5,6]. The low elastic modulus of titanium and its alloys causes lower stress accumulation than bone. So one of the most common biomedical application areas of them is the artificial hip joint replacement applications [7,8].

In the case of Ti6Al4V alloys are used as an implant material, titanium ions may accumulate locally in tissues after long-term use. However, the reaction of the bone against the implant and the success of the implant related to the chemical and physical properties of surfaces. Studies on the surface treatment of titanium are carried out to increase the bonding between the bone tissue and the implant. It is clear that reducing ion accumulation by forming stable passive TiO₂ film will provide many benefits for the patient and increase the life of the implant and prevent repeated surgeries [5,7,9,10]. This natural oxide is easily broken down and can harm the body [11]. In

addition, while titanium alloys are used in the construction of joint prostheses due to their biocompatible, durable and lightweight nature, they are not ideal for joint surfaces due to their high coefficient of friction and poor wear resistance [12]. Surface coatings with a polymer film by dip coating method is a low cost, easy to perform method, thus increasing the wear life of the component.

UHMWPE which is one of the promising polymer film, has been widely studied to improve the tribological properties of steel, aluminium and titanium substrates [4,12] and common application of this organic polymer in medicine is as hip and knee prosthetic components [13–15] because of its high corrosion and wear-resistant, biocompatibility, low coefficient of friction, good strength/ductility, self-lubricating properties compared to all other polymers [2,16,17]. Despite these superior properties of UHMWPE, wear, osteolysis and aseptic loosening caused by long-term use in hip prostheses cause bone loss, discomfort, joint loosening and limit the life of the joints [4,14,17–24]. To overcome this problem and increase the mechanical and tribological properties of UHMWPE, Hap (Ca₁₀(PO₄)₆(OH)₂) one of the attractive materials for biomedical applications can be added into the matrix. Studies have shown that the optimum amount of micro and nanoscale second phase, inorganic particles, ceramic and biomaterial reinforcement to the UHMWPE matrix can improve not only the mechanical but also the tribological properties of the UHMWPE matrix composite [19,25–29].

The objective of this study is to increase the tribological properties of Ti6Al4V substrate, which was chosen as hip joint material, and also to prevent any metal ion transfer to human body by coating with UHMWPE/Hap composite films. Microstructural and tribological properties of all UHMWPE/Hap composite film coatings will be characterized. With this study, we will also see the effect of Hap addition to the UHMWPE matrix. According to author's knowledge, this is the first reported paper investigating the effect of Hap addition on UHMWPE composite coatings over Ti6Al4V alloy for potential application of hip joint components.

Materials and methods

Preparation of samples

The UHMWPE powder having a molecular weight of 10^6 – 6.10^6 g/mol, was supplied by Sigma-Aldrich. Reinforcement agent of Hap powder was produced by biomimetic method. Decalin (decahydronaphthalene) $\geq 99\%$ was used as solvent and supplied from Alfa Aesar. Other chemicals were all purchased from Sigma-Aldrich. Ti6Al4V alloy plates with dimensions of 15 mm \times 50 mm \times 2 mm were ground in steps of 240, 320, 400, 600 and 800 grid abrasive papers to have smooth surface before anodic oxidation and cleaning process were performed in ethanol, acetone, deionized water.

Experimental studies were performed at three stages as listed below:

I. Anodic oxidation:

First anodic oxidation process of Ti6Al4V substrate has been carried out. In the electrochemical process Ti6Al4V alloy was used as anode, and a steel pot was used as cathode using a constant voltage of 100 V for 20 min. Electrolyte solution was containing of phosphoric acid and hydrogen peroxide. After oxidation process heat treatment was performed at 600°C for 1 h. Anodized and heat-treated sample surfaces were roughened and got ready for dip coating process.

II. Gellation- crystallization:

Second UHMWPE solution was prepared for dip coating process by gelation crystallization method. 3 wt-% concentration UHMWPE powder was dissolved in decalin solution by heating to 80°C for 20 min and after to 160–180°C for 45 min using magnetic stirrers. When the solution turned to transparent it indicated that dissolution was completed uniformly. UHMWPE/Hap composite gel was obtained by adding different weight ratios of Hap particles into the hot gel.

III. Dip coating:

In the third stage, anodic oxidized Ti6Al4V alloys were coated by UHMWPE-Hap composite film by dip coating process. 1.9 mm/s of dipping and withdrawal speed was used for the dip coating process with a soaking time of 75–80 s in solution. Finally, the samples were heat treated at 100°C for 20 h.

Flow chart including experimental studies was given in Figure 1.

Characterization of samples

Microstructural characterization

The chemical composition and surface morphologies of UHMWPE/Hap composite films were examined by JEOL LV6000 SEM-EDS (scanning electron microscope equipped with energy dispersive spectroscopy) and FE-SEM (Field Emission Scanning Electron Microscope).

FTIR analysis

Organic structure and the functional groups of composite coatings were analyzed by a Fourier-transformed infrared (FTIR) spectroscopy on Perkin Elmer-Spectrum in the range of 3000–500 cm^{-1} in wavelength. Three scans were applied for each sample and the average results were taken.

DSC analysis

The DSC analysis of the UHMWPE/Hap composite films was carried out by DSC (differential scanning calorimeter), TA Instruments Q20 calorimeter, under a nitrogen atmosphere. Each sample was heated to 200°C with a heating rate of 10°C/min. The melting temperature (T_m), enthalpy of fusion (ΔH_f), and degree of crystallinity (X_C) of samples were obtained by means of DSC curves. The crystallinity degree of the UHMWPE and its composites was calculated using Equation (1).

$$X_C = \frac{\Delta H_f}{\Delta H_{100}} \times 100 \quad (1)$$

(ΔH_f) represents the enthalpy of fusion and (ΔH_{100}) represents enthalpy of the crystalline UHMWPE (290 Jg^{-1}) at melting point. (ΔH_f) is determined from the area under endotherm melting peak [30].

Wear and friction tests

A tribological study of the UHMWPE-Hap composite films coated and uncoated Ti6Al4V alloys was carried out on ball-on-disk mode at a sliding speed of 12 cm/s for 6000 cycles in the mode of dry friction by CSM Instrument. Wear studies were performed against a 6 mm diameter of alumina ball, under the 2 N load in linear mode. Adhesion behaviour of composite coatings was tested via scratch tests under the 1N

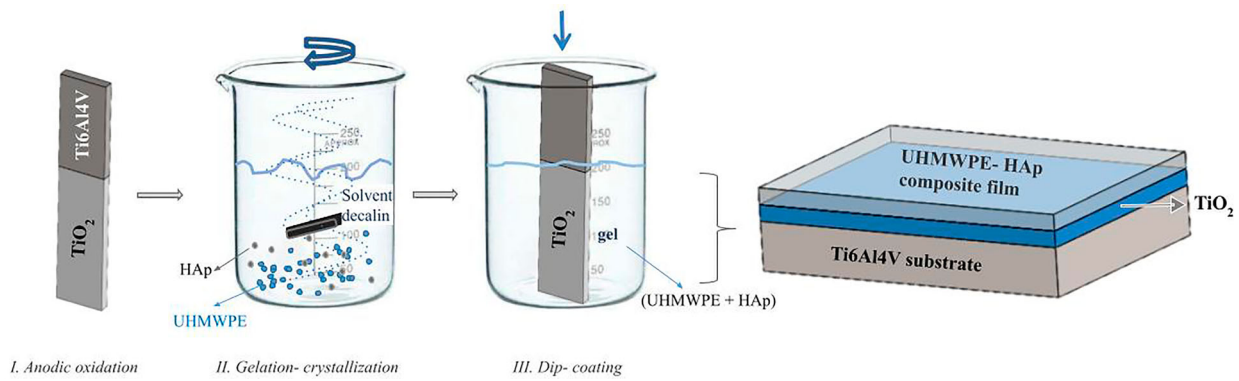


Figure 1. Process flow chart of the UHMWPE/Hap composite film coating on Ti6Al4V.

load, 0.34 cm/s sliding speed and 5 mm siliding distance in accordance with ASTM D7027 standards. KLA Tencor model 2D surface profilometer was used to analyze the worn surface and determine the wear volume.

Bioactivity tests

In this study, *in vitro* bioactivity examination of UHMWPE-Hap composite coatings was performed by soaking specimens in nonconventional simulated body fluid (SBF) solution. The ionic composition of blood plasma and SBF solution was given in Table 1. While preparing the SBF, the pH was set to 7.4 using hydroxymethyl aminomethane (TRIS) and 1.0 M HCl to prevent precipitation, and the reagents were added after the dissolution process in the 700 mL of water. The biomimetic process in SBF is based on the precipitation of heterogeneous calcium phosphate nucleation formed in SBF (synthetic body fluid) at 37°C and 7.4 pH. Synthetic body fluid is prepared as a result of chemical analysis of human body fluid. Its concentration is adjusted equal to the human blood plasma. Biomineralization by depositing bone-like apatite in the prepared SBF was carried out in a water bath of 37°C. Since the apatite formed on the surface will consume the phosphate ions and calcium ions, therefore, synthetic body fluid is renewed at regular intervals. Bone-like apatite deposition was achieved on the surface of UHMWPE/Hap composite materials by keeping them in SBF environment at body temperature for 8 days and characterized by SEM-EDS.

Surface wettability

Contact angle tests were performed for determining the hydrophilicity and biocompatibility of UHMWPE-Hap composite coatings with the human

body before and after keeping them in SBF solution by using Attention Optical Tensiometer measuring device. The pendant drop method was used for contact angle analysis by dripping microliter distilled water on the substrate surfaces. Before this process, the contact angle device was calibrated, and the substrate was made flat.

Results and discussion

UHMWPE-Hap composites were coated on anodic oxidized Ti6Al4V alloy homogeneously by dip coating method. Microstructures of UHMWPE/Hap composite films were first examined by SEM. Figure 2 shows SEM microstructures of UHMWPE-Hap composite coatings with the unreinforced UHMWPE. Grey dimpled regions belong to UHMWPE matrix, and rare white small dots indicate the Hap particles. The Hap particles were surrounded and tightly bound by the polymer matrix and dispersed homogeneously in the UHMWPE matrix. Although interfaces were defect-free.

Microstructures of UHMWPE/Hap composite films were investigated in detail by FESEM (Figure 3). It is seen from the microstructures that the composite coatings have a homogeneous, dense porous and fibrous structure composed of UHMWPE lamellar chains connected to each other by fibrils having macrovoids. The diameter of macrovoids is approximately 3–5 µm, and the pore diameters decreased with the addition of Hap particles, and the structure has become more homogenous. At higher magnifications lamellar structure and grain boundaries of UHMWPE matrix are seen obviously (Figure 4).

Homogenous distribution of Hap particles in UHMWPE matrix and perfect bonding between them provided superior properties. We suggested

Table 1. Ion concentration of blood plasma and SBF solution.

Ion (mM)	Na ⁺	K ⁺	Mg ²⁺	Ca ²⁺	Cl ⁻	HPO ₄ ²⁻	SO ₄ ²⁻	HCO ₃ ⁻
Blood	142.0	5.0	1.5	2.5	103.0	1.0	0.5	27.0
SBF	142.0	5.0	1.5	2.5	147.8	1.0	0.5	4.2

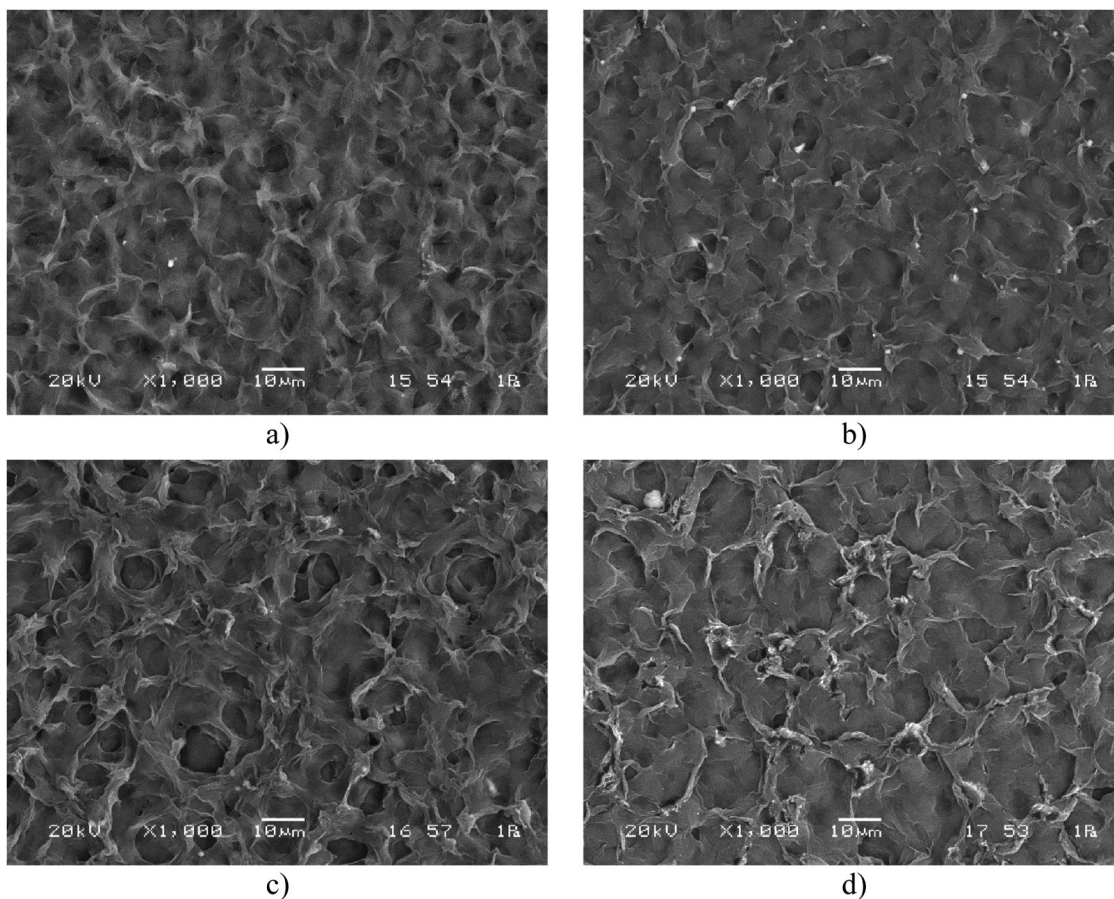


Figure 2. SEM images of (a) pure UHMWPE, (b) UHMWPE/0.5wt-%Hap, (c) UHMWPE/1wt-%Hap and (d) UHMWPE/2wt-%Hap composite films.

that gelation crystallization method ensured the dispersion of Hap particles homogeneously and caused the heterogeneous nucleation by attaching UHMWPE chains on them. Therefore, UHMWPE-Hap composites have higher crystallinity than unreinforced UHMWPE. Furthermore, SEM and FESEM results showed that the surface of UHMWPE-Hap composite coating became more homogeneous and less wrinkled in relation to the smaller size of macro voids with increasing the amount of Hap particles. A decrease in the size of macro voids can be based on the increased nucleation agent of Hap particles by connecting each other with the polymer chains. It is possible to say that, increased bonds will increase the crystallinity degree and therefore mechanical properties of UHMWPE/Hap composites will increase positively similar to studies done by Senatov [31] and Maksimkin et al. [32]. In other words, the adhesion of Hap particles with the polyethylene matrix will increase the mechanical properties of the composite.

Elemental analysis and mapping were carried out through SEM-EDS in order to estimate the atomic composition of composite coating (Figures 5 and 6). The results revealed that white regions in Figure 5 including Ca, P and O elements indicate the hydroxyapatite particles. It was found that the atomic ratio of Ca/P is approximately 1.65 which proves the presence

of hydroxyapatite. As can be seen in the SEM-Map analysis (Figure 6) Ca, P and O are found together and dispersed homogeneously in the UHMWPE matrix.

Mechanical properties and wear resistance of UHMWPE composites highly depend on the chemical properties, crystalline-amorphous phase amount and the reinforcing particle distribution of composite. FTIR analyses of pure UHMWPE, UHMWPE-0.5, 1 and 2wt-%Hap composite coatings, treated with IR rays to get an idea about their special chemical bonds, are illustrated in Figure 7. The characteristic absorption peaks for phosphate group (PO_4^{3-}) of Hap are observed in the range 561 and 610 cm^{-1} (ν_4), between 1033 and 1074 cm^{-1} (ν_3), and at 957 cm^{-1} (ν_1) which are attributed to P-O bending, asymmetric P-O stretching and symmetric P-O stretching vibrations, respectively. Three basic peaks for UHMWPE could be found. As shown in Figure 7 two strong peaks at 2846 and 2915 cm^{-1} correspond to CH stretching modes, peaks at 1458 – 1469 cm^{-1} corresponding to the bending of $-\text{CH}_2-$ and the peaks at 718 – 732 cm^{-1} attributes to CH_2 rocking vibration. With the addition of Hap other peaks appeared at the 1645 cm^{-1} and 1735 cm^{-1} are attributed to C=C stretching vibration [33] and C=O bonds [20], respectively. All characteristic peaks of both

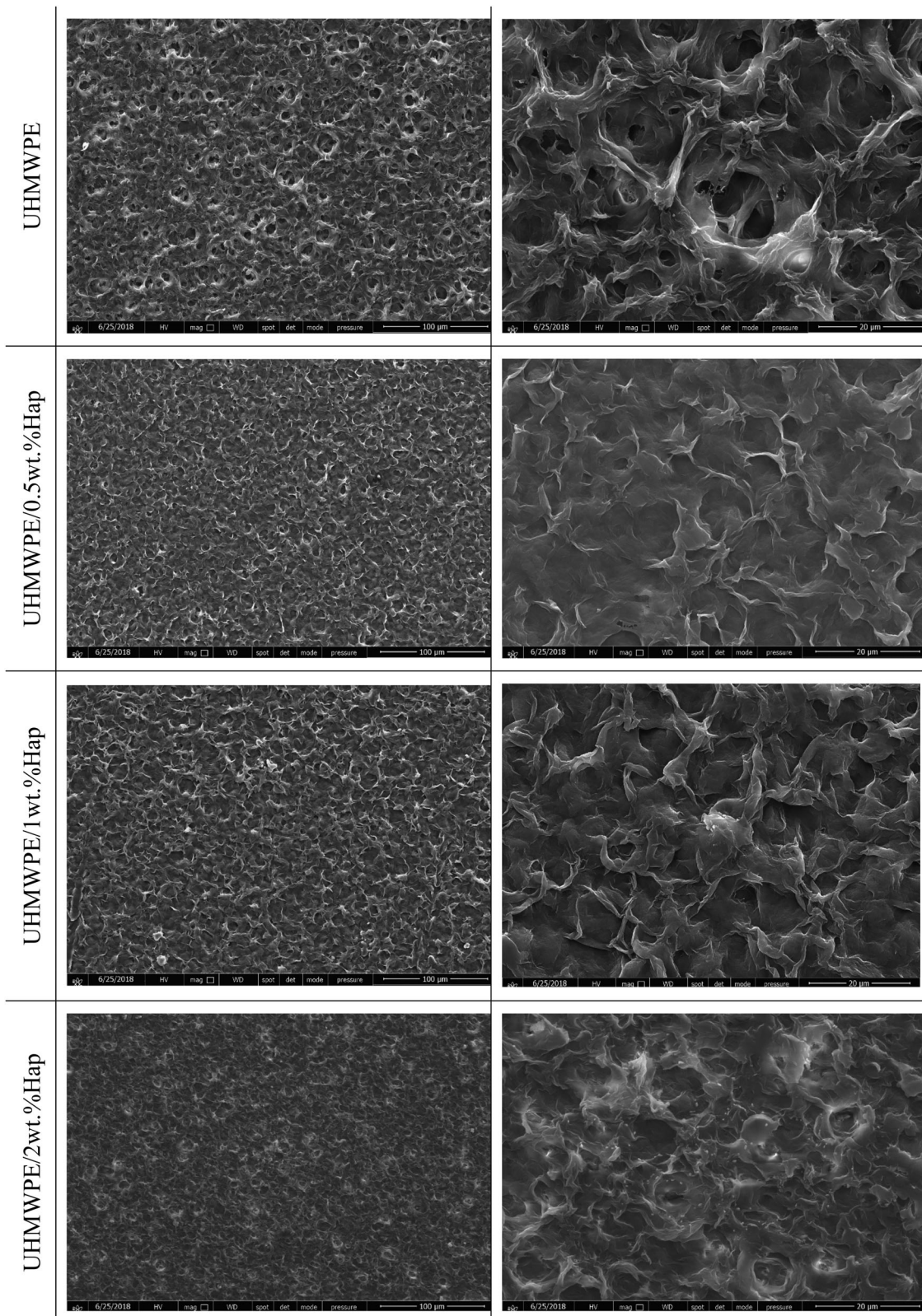


Figure 3. FE-SEM images of UHMWPE/Hap composite films, 100 \times (left column) and 5000 \times (right column).

Hap and UHMWPE structures were determined with the FTIR results, and their structures were confirmed compatible with literature. Chemical groups identified by FTIR are evidence of homogenous distribution of reinforcement particles into the UHMWPE matrix. Increasing intensity of all peaks with increasing Hap particles can be attributed to increasing bond strength

between UHMWPE chains and Hap, and it brings increasing the crystalline phase amount. UHMWPE has small hydrogen side groups, which cause high chain mobility.

Effect of Hap addition on the crystallinity degree of UHMWPE was detected by DSC analysis. [Figure 8](#) shows the DSC curves of the UHMWPE composites.

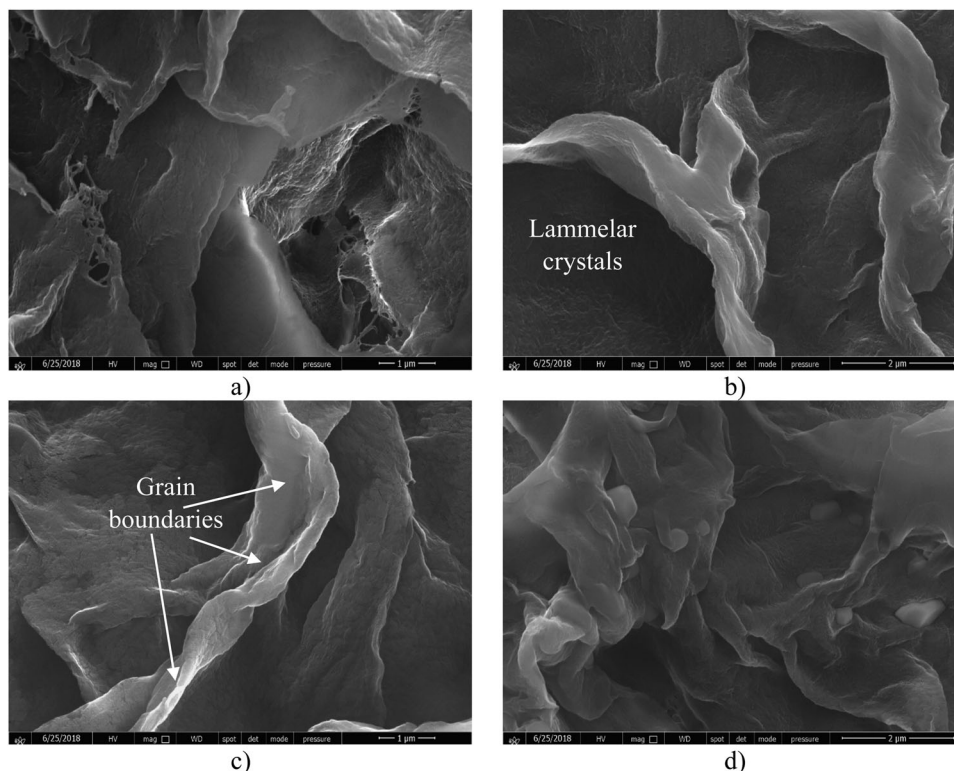


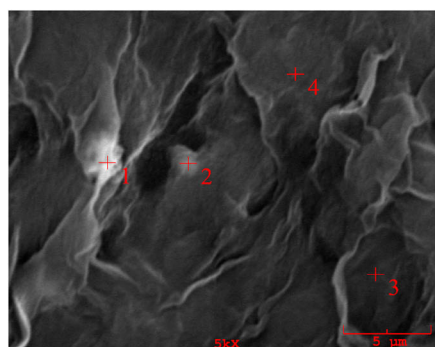
Figure 4. FE- SEM images of (a) UHMWPE, (b) UHMWPE/0.5wt-%Hap, (c) UHMWPE/1wt-%Hap and (d) UHMWPE/2wt-%Hap composite films, 50.000 \times .

Figure 8 shows that there are distinct endotherm peaks showing the melting points (T_m) of the composites which are approximately 140°C for pure UHMWPE. The addition of Hap increased the T_m of UHMWPE-Hap composites. There is an apparent increase in T_m at 2 wt-% of Hap addition.

Table 2 shows the DSC data results for UHMWPE-Hap composites. The addition of Hap increased both T_m and the crystallinity degree of UHMWPE significantly.

Any barrier to chain movement can increase the degree of crystallinity and also the strength of polyethylene by means of crosslinking between the chains [34]. As a study done by Chang et al. showed that reinforcement can increase or decrease the nucleation of polymer depending on its chemical properties. In this study, the increment of both the melting point

and 130% of crystallinity for UHMWPE-2wt-%Hap composite was achieved. This is related to the arrangement in chain folding orientation [35] enhancing chain mobility and increasing bond strength. As Chang et al. [15] claimed in their study, nonhomogeneous dispersion and the agglomeration of reinforcement can cause abrasive wear by the detachment of fillers easily. Therefore, obtaining an optimum level and homogenous dispersion of filler has a positive effect on the wear mechanism of UHMPE matrix composites. It is obviously known that fillers in the polymer matrix composites act as load-bearing agent [36]. In our study homogenous distribution of Hap particles had favourable effect on wear properties. Wear traces of UHMWPE-Hap composite films were analyzed by SEM (Figure 9). In general, pure UHMWPE has significant folds perpendicular to the



Elements	wt.%			
	Mark 1	Mark 2	Mark 3	Mark 4
C	52.67	70.09	86.4	77.2
O	32.35	21.75	12.11	21.8
P	5.58	3.49	1.18	0.6
Ca	9.39	4.67	0.28	0.36

Figure 5. SEM-EDS analyzes of UHMWPE/0.5wt-%Hap composite film.

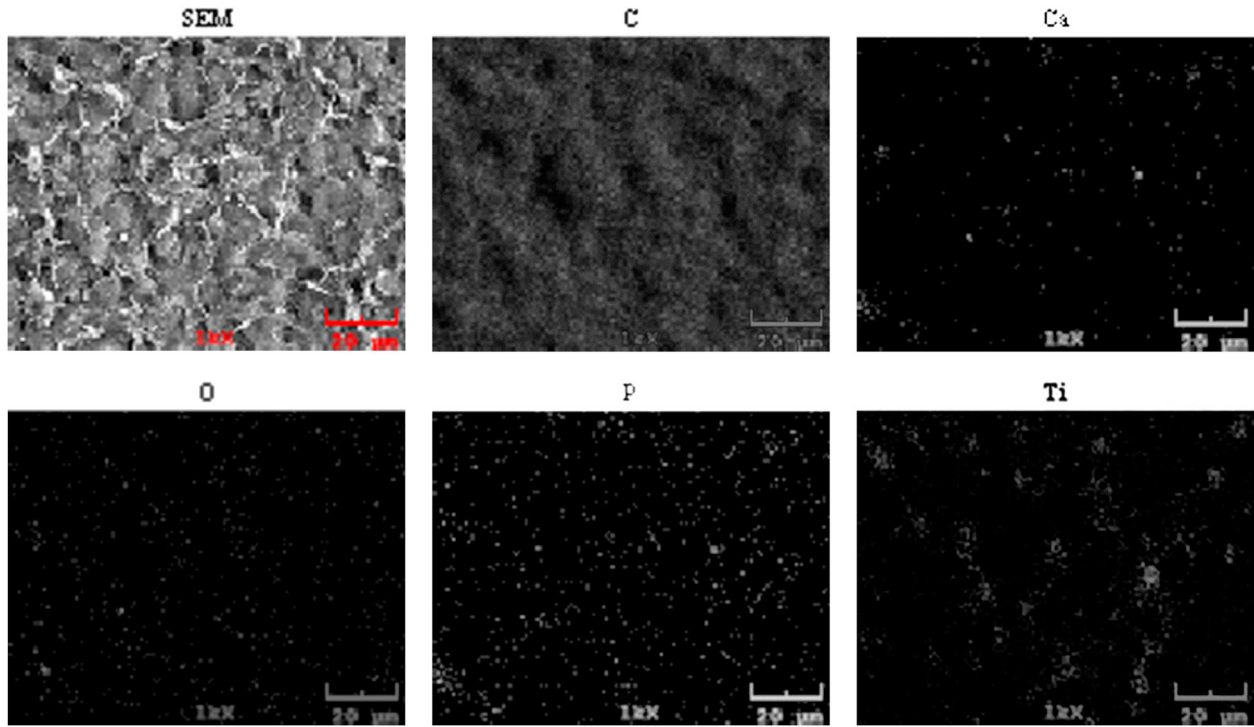


Figure 6. SEM-EDS map analyzes of UHMWPE/1wt-%Hap composite film.

wear trace and the wear mechanism occurs by creeping and folding of the polymer in adhesive character. Plastic deformation decreases with increasing Hap amount. Figure 9 shows that scar width significantly decreased with the addition of 2wt-% of Hap particles.

Worn surface images of UHMWPE-Hap composite coatings at higher magnification were given in Figure 10. White regions are Hap-rich zones, and it is seen that they dispersed homogeneously in the matrix. Plastic deformation folds are clearly seen for pure UHMWPE coating and the size and depth of these folds and the plastic deformation decreases as the Hap addition to UHMWPE matrix.

Variation of the friction coefficient of pure UHMWPE, and UHMWPE-Hap composite coated and as well uncoated Ti6Al4V alloy is shown in Figure 11. The friction coefficient of pure UHMWPE started with a value of 0.4 at the beginning and during the

wear test reached a steady state with a friction coefficient of 0.55. As is seen in Figure 11 the friction coefficient of UHMWPE dropped to 0.02 with the addition of Hap. It is possible to claim that Hap addition decreases the friction coefficient of UHMWPE significantly. Test results showed that higher crystallinity resulted in lower friction coefficient and increased wear resistance. With the addition of the 2wt.Hap powders to the UHMWPE, a drastic decrease of friction coefficient was observed (96%) and also wear resistance improved noticeably, compared to the purely UHMWPE sample. A decrease in friction coefficient with increased crystallinity could be related to the increased storage modulus caused by the increased crystallinity. It can be said that adhesive wear is the main mechanism. After each test, any deep grooves and micro-cuttings were not found on the surface. As Aliyu et al. claimed in their study that this is related to the self-lubrication effect of UHMWPE matrix [37]. Folds on the worn surfaces of composite film coatings appeared to be smaller with the addition of Hap, and the degree of plastic deformation was observed to be reduced with a smoother worn surface which will probably cause a reduction in the wear rate. This can be related to the better load carrying capability of UHMWPE-Hap composite coatings in comparison to pure UHMWPE. As Tong et al. reported in their study, reinforcements improve the bond strength at the interface [38] and increase the wear properties. Many studies revealed that wear resistance of a polymer is relevant to its mechanical properties in connection with crystallinity. Hence, higher crystallinity gives higher elastic modulus and yield strength [39].

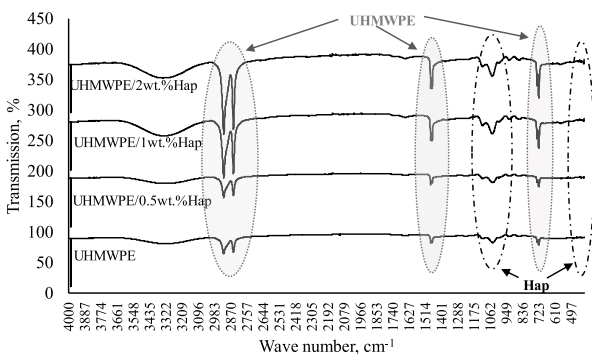


Figure 7. FTIR spectra of UHMWPE/Hap composite films.

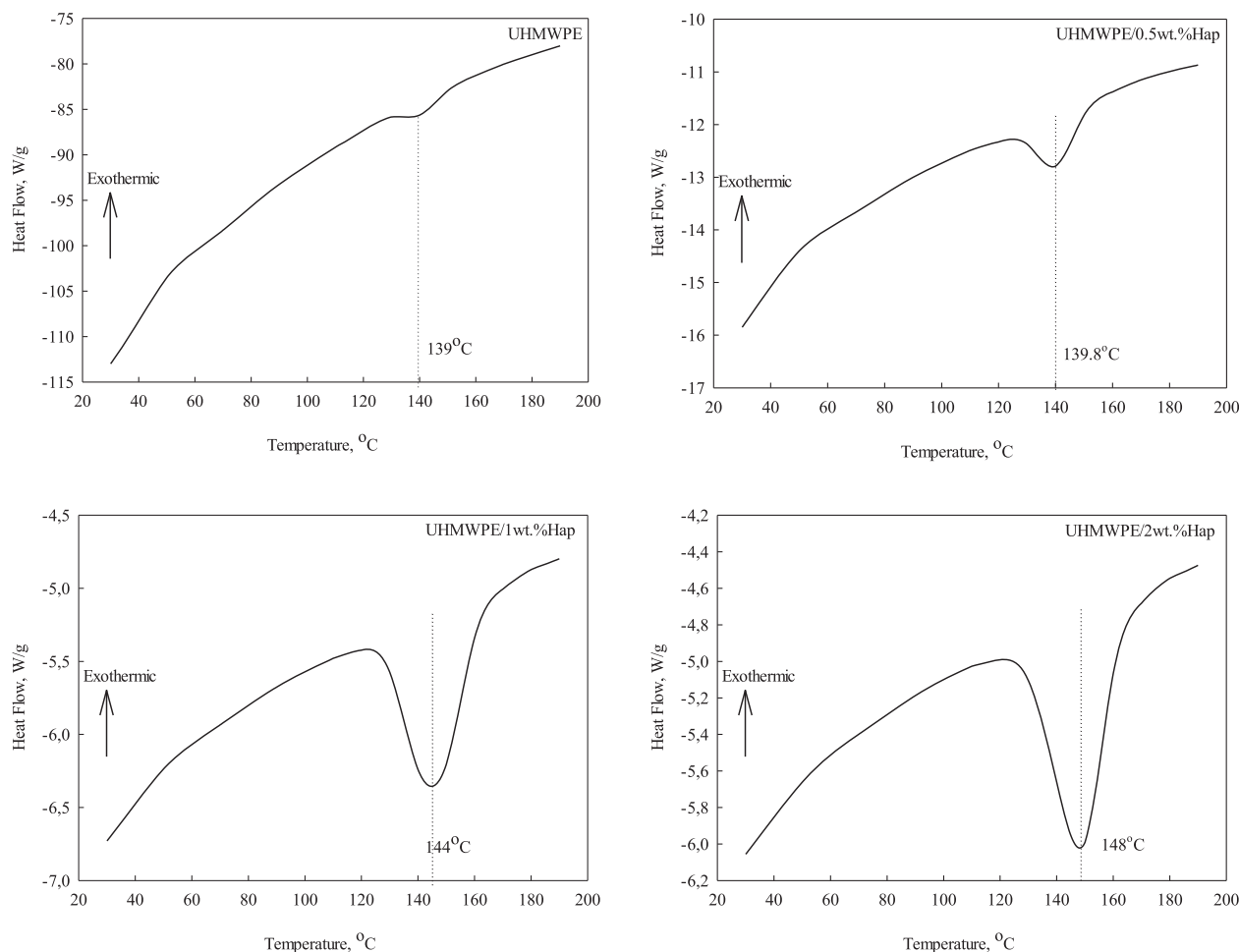


Figure 8. DSC curves of UHMWPE and UHMWPE/Hap composite films.

Worn surfaces of UHMWPE/Hap composite films including uncoated Ti6Al4V were analyzed by 2D surface profilometer and their graphs were given in Figure 12.

Worn area given by profilometer and friction coefficient variation of uncoated (anodic oxidized) Ti6Al4V alloy and UHMWPE-Hap composites versus wt-% of Hap was illustrated in Figure 13. The worn track area gives information about the wear performance. The smaller the worn area, the higher the wear resistance. The worn area of UHMWPE-2wt-%Hap composite was 78 times lower than the uncoated (anodic oxidized) Ti6Al4V alloy and also 22 times lower than the pure UHMWPE coating. The above results showed that the reinforcing with Hap particles increases the mechanical and wear properties of composite coating film on Ti6Al4V. As it was seen in SEM results (Figure 2–3), this is the consequence of

decreasing micro asperities by means of Hap addition similar to the study done by Pina et al. [40].

SEM microstructures of UHMWPE/Hap composite films after immersion in SBF solution for 8 days were given in Figure 14.

It is seen from Figure 14 that, flower-like plates accumulated on the surfaces of all composite coatings homogeneously. Elemental analysis of this accumulation was performed by SEM-EDS analysis. EDS results given in Figure 15 showed that flower-like plates include Ca, P and O elements which are the main components of Hap. Considering the Ca/P ratio, it can be said that these deposits belong to brushite, which is the precursor phase of Hap. This result shows that brushite can be transformed into Hap if the immersion time is increased. Studies done by Macuvele et al. indicated that the growth of Hap increases with the increasing immersion time [28]. Any accumulation out of Hap was not observed on the surface of the test materials during immersion of test materials in the SBF.

Water contact angle measurements were performed on the surfaces of the UHMWPE/Hap composite films before and after immersion in SBF solutions and the results were given in Table 3. It is observed that the water contact angle decreased with the Hap content both before and after immersion in SBF.

Table 2. DSC results of UHMWPE/Hap composites including T_m , ΔH_f and X_c .

Sample	T_m (°C)	ΔH_f (Jg ⁻¹)	X_c (%)
UHMWPE	139	71.1	25
UHMWPE/0.5wt-%Hap	139.8	100.3	35
UHMWPE/1wt-%Hap	144	157.1	54.30
UHMWPE/2wt-%Hap	148	164.4	56.8

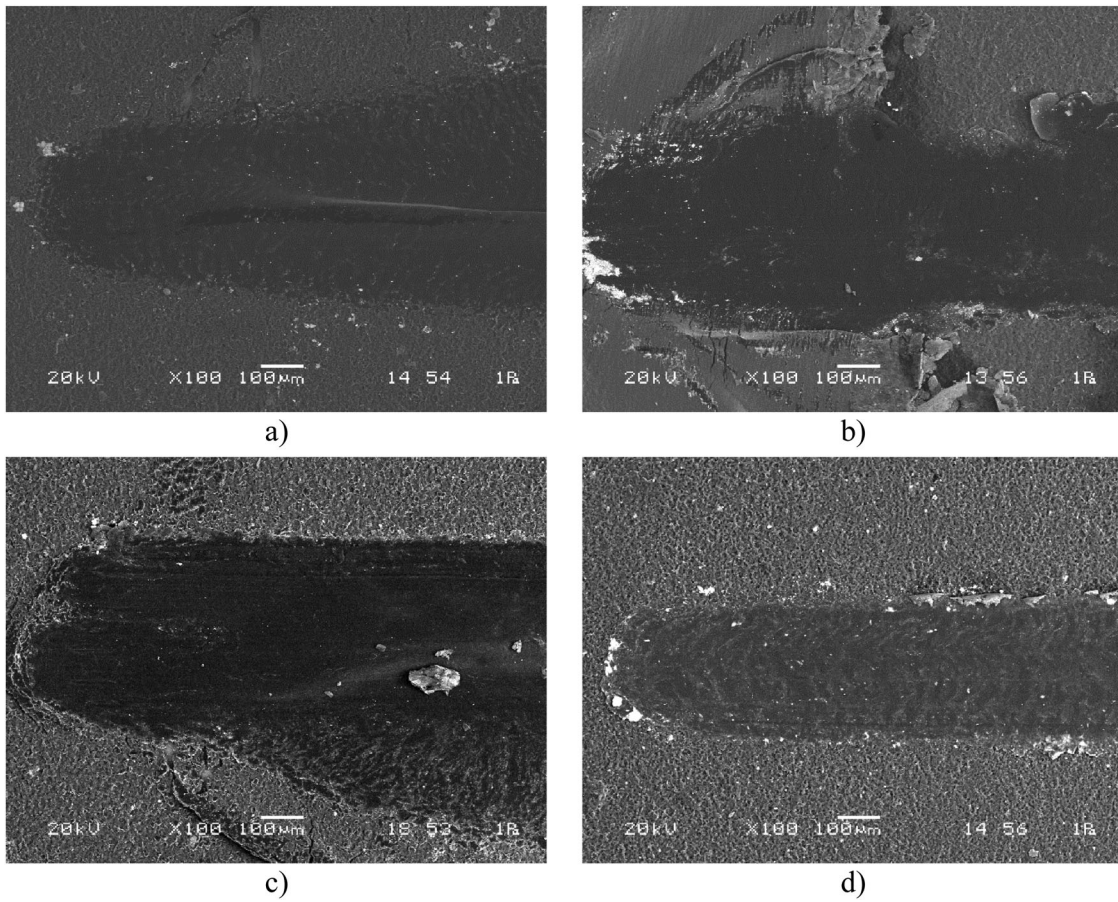


Figure 9. (a) SEM images of origin of the wear traces for pure UHMWPE, (b) UHMWPE/0.5wt-%Hap, (c) UHMWPE/1wt-%Hap and (d) UHMWPE/2wt-%Hap composite films.

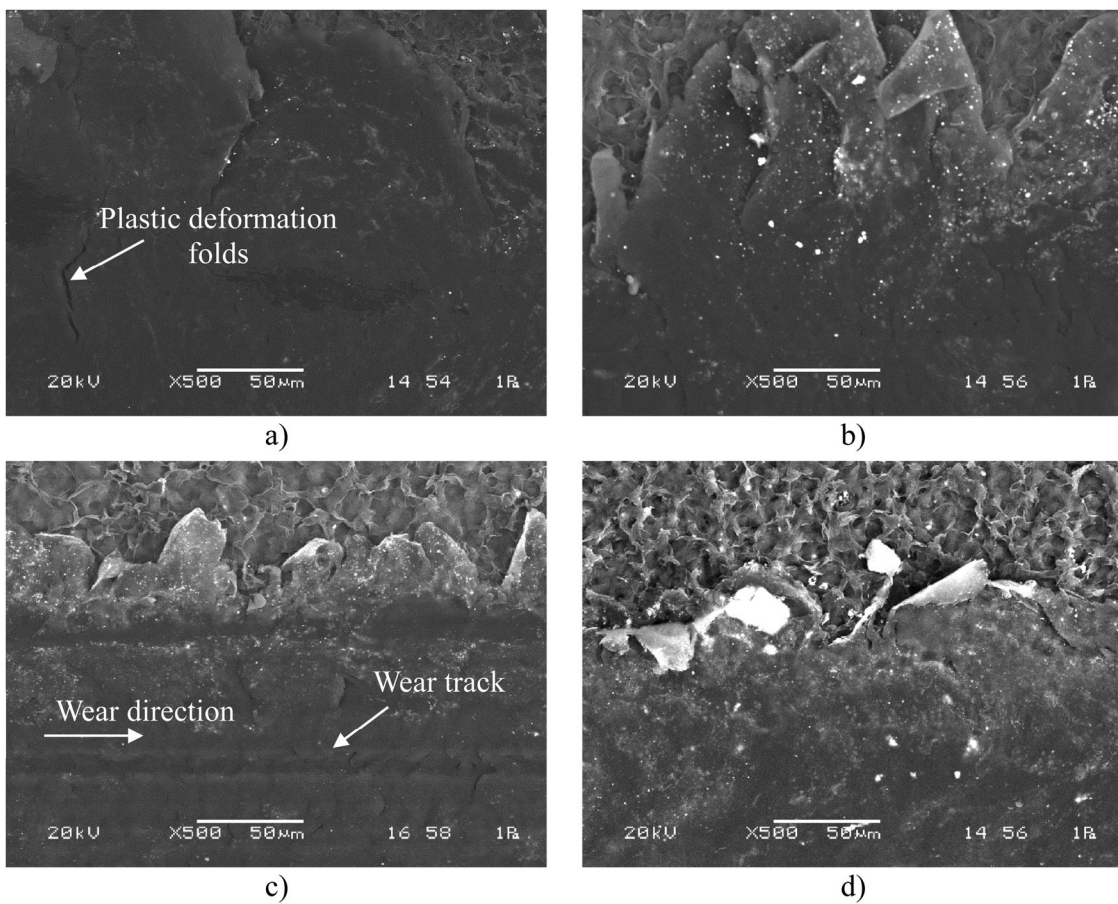


Figure 10. (a) SEM images of wear traces of pure UHMWPE (top), (b) UHMWPE/0.5wt-%Hap, (c) UHMWPE/1wt-%Hap and (d) UHMWPE/2wt-%Hap composite films.

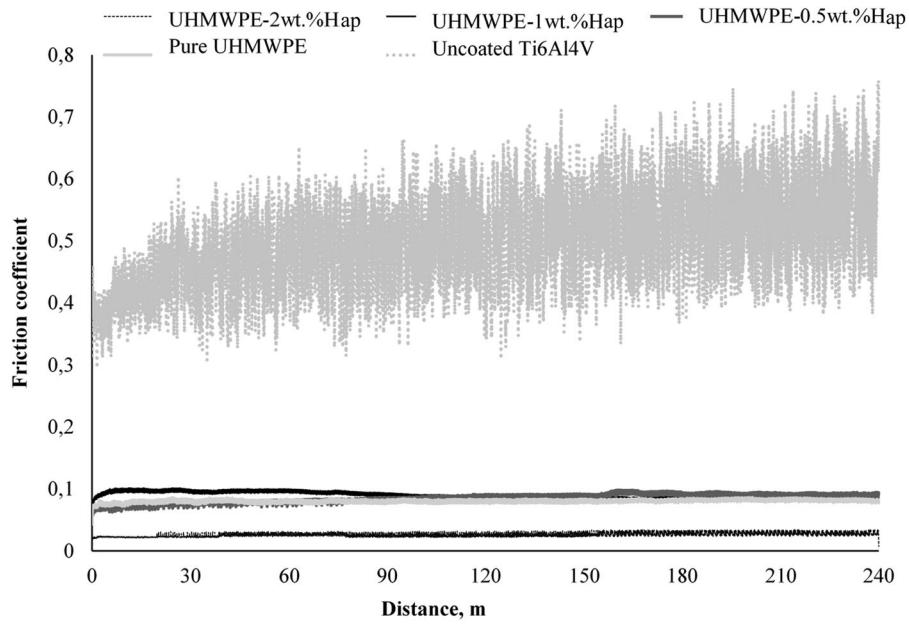


Figure 11. Friction coefficient of UHMWPE/Hap composite films including uncoated oxidized Ti6Al4V.

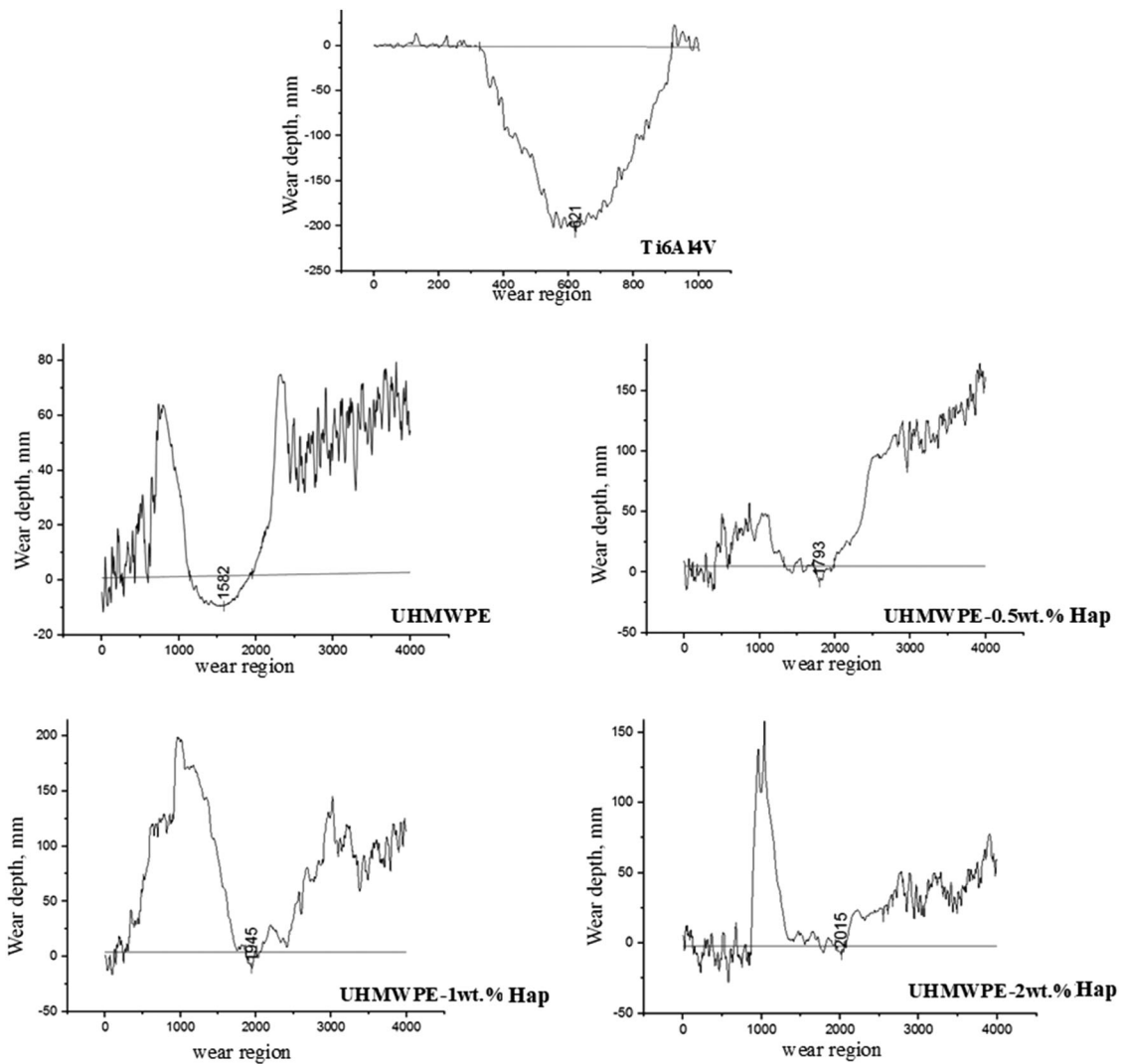


Figure 12. 2D profilometer graphs of UHMWPE/Hap composite films with uncoated oxidized Ti6Al4V.

The water contact angle of UHMWPE film is determined as 103° and decreased to 98, 94 and 88° for the 0.5, 1 and 2wt-% reinforced composite coatings,

respectively before the immersion in SBF. After immersion in SBF solution water contact angle for the UHMWPE film was determined as 82° and

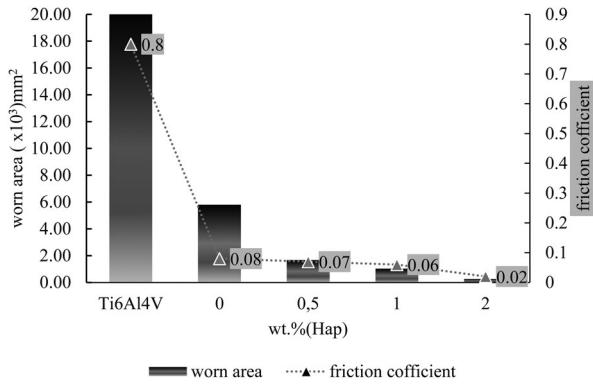


Figure 13. Worn area and friction coefficient variation of uncoated Ti6Al4V alloy and UHMWPE/Hap composite films versus Hap addition.

decreased to 60° with the addition of 2wt-% Hap. The decrement in the contact angle values indicates the increasing hydrophilic character [41].

Hap addition to UHMWPE not only increases the mechanical properties but also makes easy the biological adsorption on tissue [28]. We performed *in vitro* tests in SBF solutions. It was observed that with an increasing amount of Hap particles and also with the immersion in SBF solution, the surface of the composite coating became more hydrophilic related to the increasing surface roughness. Tihan et al. investigated the hydrophilic–hydrophobic balance on biocompatibility of polymethyl methacrylate–hydroxyapatite composites via contact angle test. Their results showed

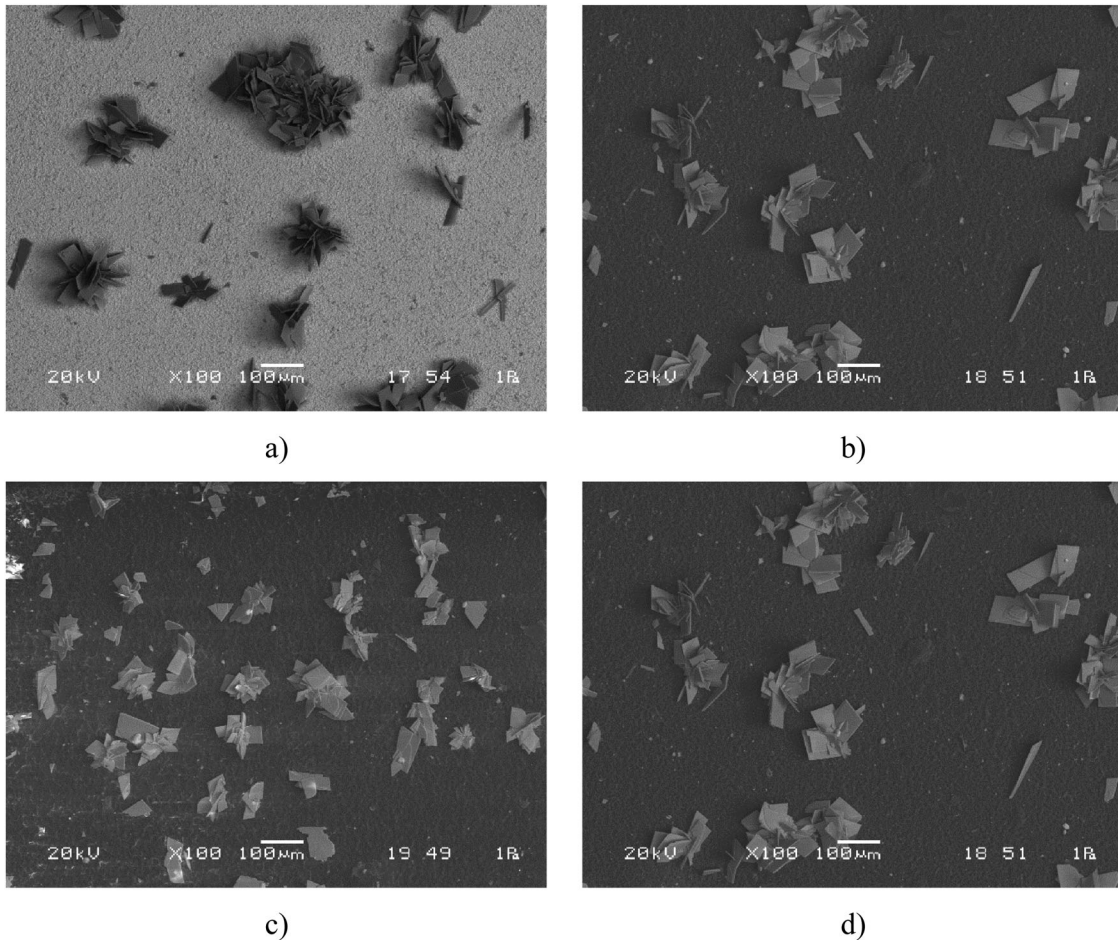
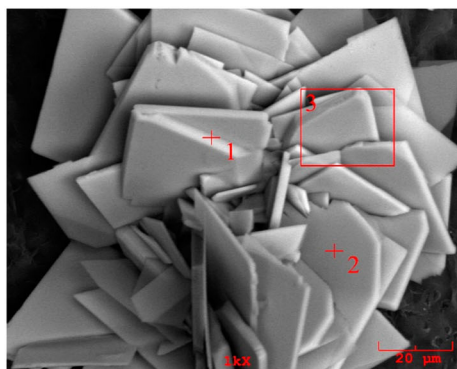




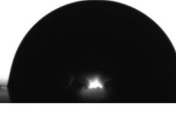
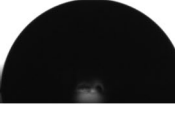


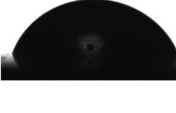

Figure 14. SEM microstructures of (a) pure UHMWPE, (b) UHMWPE/0.5wt-% Hap, (c) UHMWPE/1wt-%Hap and (d) UHMWPE/2wt-%Hap composite films after immersion in SBF solution.



Elements	Mark 1	Mark 2	Mark 3
C	6.59	9.96	7.65
O	54.71	44.44	42.5
P	17.79	13.72	23.6
Ca	20.29	24.07	26.2

Figure 15. SEM-EDS analysis of UHMWPE-0.5wt-% Hap composite coating after immersion in SBF solution.

Table 3. Water contact angle measurements of UHMWPE and UHMWPE/Hap composite films before and after immersion in SBF. Contact angle, °

	UHMWPE	UHMWPE-0.5wt.%Hap	UHMWPE-1wt.%Hap	UHMWPE-2wt.%Hap
Before SBF	103 	98 	94 	88 
After SBF	82 	73 	70 	60 

that contact angle of composites decreased with increasing amount of Hap particles similar to our results which implies the increment of hydrophilic character leading to good cell growth [42].

Hydrophilic surfaces are beneficial for improving wear properties. The reduction in contact angles will have a favourable effect *in vivo*, as it will provide more interaction with body fluids in the relevant region in the body environment.

Conclusions

- In this study, both the porous TiO₂ and UHMWPE-Hap composite film coating processes were performed successfully to improve the chemical, tribological and biological properties of Ti6Al4V alloy by anodic oxidation and dip coating method, respectively.
- SEM and FESEM studies showed that composite coatings were homogenous and continuous. Homogenous dispersion of Hap particles in UHMWPE matrix was detected via SEM-EDS analysis. Furthermore, the existence of Hap particles was proved by FTIR analysis.
- DSC studies showed us that the melting points and herewith bond strength of composites increased by the addition of Hap particles.
- The addition of Hap not only increased the melting point and crystallinity degree but also the wear resistance of UHMWPE.
- Increasing crystallinity brings about both ultra-low friction coefficient of 0.02 and excellent wear durability with a decrease of 98% of the worn area for UHMWPE-2wt-%Hap composite coating.
- Hap additions to the UHMWPE matrix also increased the hydrophilicity which is the evidence of biocompatibility. Hence, the UHMWPE-2wt-% Hap composite coating on anodic oxidized Ti6Al4V can be a potential nominee for Hip joint prosthesis.

Disclosure statement

No potential conflict of interest was reported by the author(s).

References

- [1] Moreno SS. Carbon reinforced UHMWPE composites for orthopaedic applications characterization and biological response to wear particles, 2013. Available from: <https://www.diva-portal.org/smash/get/diva2:999533/FULLTEXT01.pdf>
- [2] He W, Benson R. 10 polymeric biomaterials. Applied Plastics Engineering Handbook, Elsevier; 2011. doi:10.1016/B978-1-4377-3514-7.10010-8
- [3] Pekşen C, Doğan A. Implant permanence. TOTBİD. 2011;10:122–128.
- [4] Ghosh S, Abanteriba S. Status of surface modification techniques for artificial hip implants. Sci Technol Adv Mater. 2016;17:715–735. doi:10.1080/14686996.2016.1240575
- [5] He DH, Wang P, Liu P, et al. HA coating fabricated by electrochemical deposition on modified Ti6Al4V alloy. Surf. Coatings Technol. 2016;301:6–12. doi:10.1016/j.surfcoat.2016.07.005
- [6] Panjwani B, Satyanarayana N, Sinha SK. Tribological characterization of a biocompatible thin film of UHMWPE on Ti6Al4V and the effects of PFPE as top lubricating layer. J Mech Behav Biomed Mater. 2011;4:953–960. doi:10.1016/j.jmbbm.2011.02.005
- [7] Bigdeli I, Haft Asia MN, Miladi-Gorji H, et al. Surface modification of titanium, titanium alloys, and related materials for biomedical applications. Mater Sci Eng R. 2004;47:49–121. doi:10.1016/j.mser.2004.11.001
- [8] Elias CN, Lima JHC, Valiev R, et al. Biomedical applications of titanium and its alloys. Jom. 2008;60:46–49. doi:10.1007/s11837-008-0031-1
- [9] Cely MM, Toro A, Estupiñan H, et al. Microstructure characterization and tribological behavior of anodized ti6al4v alloy. Ing y Compet. 2014;16:295–305.
- [10] Wang G, Li J, Lv K, et al. Surface thermal oxidation on titanium implants to enhance osteogenic activity and *in vivo* osseointegration. Sci Rep. 2016;6:1–13. doi:10.1038/srep31769
- [11] Vera ML, Rosenberger MR, Schvezov CE, et al. Fabrication of TiO₂ crystalline coatings by combining Ti-6Al-4V anodic oxidation and heat treatments. Int J Biomater. 2015;2015:1–9. doi:10.1155/2015/395657

- [12] Wang K, Xiong D, Deng Y, et al. Ultra-lubricated surface of Ti6Al4V fabricated with combination of porous TiO₂ layer, ultra-high molecular weight polyethylene film and hydrophilic polymer brushes. *Mater Des.* 2017;114:18–24. doi:10.1016/j.matdes.2016.10.032
- [13] Minn M, Sinha SK. DLC and UHMWPE as hard / soft composite film on Si for improved tribological performance. *Surf Coat Technol.* 2008;202:3698–3708. doi:10.1016/j.surfcoat.2008.01.012
- [14] Valenza A, Visco AM, Torrisi L, et al. Characterization of ultra-high-molecular-weight polyethylene (UHMWPE) modified by ion implantation. *Polymer (Guildf.)* 2004;45:1707–1715. doi:10.1016/j.polymer.2003.12.056
- [15] Chang B-P, Md H, Akil R, et al. Comparative study of micro- and nano-ZnO reinforced UHMWPE composites under dry sliding wear. *Wear.* 2013;297:1120–1127. doi:10.1016/j.wear.2012.11.083
- [16] Ramakrishna S, Mayer J, Wintermantel E, et al. Biomedical applications of polymer-composite materials: a review. *Compos Sci Technol.* 2001;61:1189–1224.
- [17] Kurtz SM, Ph D. The required mechanical properties of hip and knee components. Available from: <https://www.researchgate.net/publication/228965764>, 2003 50–59.
- [18] Cohen, Y., Rein, D. M., & Vaykhansky, L. Departmenty. A novel composite based on ultra-high-molecular-weight polyethylene. *Compos Sci Technol.* 1997;3538:1149–1154.
- [19] Liu J, Zhu Y, Wang Q, et al. Biotribological behavior of ultra high molecular weight polyethylene composites containing bovine bone hydroxyapatite. *J China Univ Min Technol.* 2008;18:606–612. doi:10.1016/S1006-1266(08)60303-X
- [20] Pang W, Ni Z, Chen G, et al. Mechanical and thermal properties of graphene oxide/ultrahigh molecular weight polyethylene nanocomposites. *RSC Adv.* 2015;5:63063–63072. doi:10.1039/c5ra11826c
- [21] Aoiike T, Yokoyama D, Uehara H, et al. Tribology of ultra-high molecular weight polyethylene disks molded at different temperatures. *Wear.* 2007;262:742–748. doi:10.1016/j.wear.2006.08.006
- [22] Gonzalez-Mora V, Hoffmann M, Chiesa R, et al. Screening wear tester versus hip joint simulator: results of UHMWPE sliding against different CoCrMo counterfaces. *Surf Eng.* 2003;19:45–50. doi:10.1179/026708403225002478
- [23] Epstein NJ, Bragg WE, Ma T, et al. UHMWPE wear debris upregulates mononuclear cell proinflammatory gene expression in a novel murine model of intramedullary particle disease. *Acta Orthop.* 2005;76:412–420. doi:10.1080/17453670510041321
- [24] Pietrzak WS. Ultra-high molecular weight polyethylene for total Hip acetabular liners: a brief review of current status. *J Investig Surg.* 2021;34:321–323. doi:10.1080/08941939.2019.1624898
- [25] Guofang G, Huayong Y, Xin F. Tribological properties of kaolin filled UHMWPE composites in unlubricated sliding. *Wear.* 2004;256:88–94. doi:10.1016/S0043-1648(03)00394-6
- [26] Fang L, Leng Y, Gao P. Processing of hydroxyapatite reinforced ultrahigh molecular weight polyethylene for biomedical applications. *Biomaterials.* 2005; 26:3471–3478. doi:10.1016/j.biomaterials.2004.09.022
- [27] Tong J, Ma Y, Jiang M. Effects of the wollastonite fiber modification on the sliding wear behavior of the UHMWPE composites. *Wear.* 2003;255:734–741. doi:10.1016/S0043-1648(03)00221-7
- [28] Macuvele DLP, Nones J, Matsinhe JV, et al. Advances in ultra high molecular weight polyethylene/hydroxyapatite composites for biomedical applications: A brief review. *Mater Sci Eng C.* 2017;76:1248–1262. doi:10.1016/j.msec.2017.02.070
- [29] fang An M, jun Xu H, Lv Y, et al. The influence of chitin nanocrystals on structural evolution of ultra-high molecular weight polyethylene/chitin nanocrystal fibers in hot-drawing process. *Chin J Polym Sci. (English Ed.)* 2016;34:1373–1385. doi:10.1007/s10118-016-1843-z
- [30] Kong Y, Hay JN. The measurement of the crystallinity of polymers by DSC. *Polymer (Guildf.)* 2002;43:3873–3878.
- [31] Senatov FS, Baranov AA, Muratov DS, et al. Microstructure and properties of composite materials based on UHMWPE after mechanical activation. *J Alloys Compd.* 2015;615:S573–S577. doi:10.1016/j.jallcom.2013.12.175
- [32] Maksimkin AV, Nematulloev SG, Chukov DI, et al. Bulk oriented UHMWPE/FMWCNT films for tribological applications. *Polymers (Basel).* 2017;9:1–12. doi:10.3390/polym9110629
- [33] Feng M, Li W, Liu X, et al. Copper-polydopamine composite coating decorating UHMWPE fibers for enhancing the strength and toughness of rigid polyurethane composites. *Polym Test.* 2021;93:106883, doi:10.1016/j.polymertesting.2020.106883
- [34] Whitesides GM, Wong AP. The intersection of biology and materials science. *MRS Bull.* 31;2006:19–27. doi:10.1557/mrs2006.2
- [35] Peng Chang B, Md Akil H, Bt Nasir R, et al. Optimization on wear performance of UHMWPE composites using response surface methodology. *Tribol Int.* 2015;88:252–262. doi:10.1016/j.triboint.2015.03.028
- [36] Zhenhua L, Yunxuan L. Mechanical and tribological behaviour of UHMWPE/HDPE blends reinforced with SBS. *Polym - Plast Technol Eng.* 2012;51:750–753. doi:10.1080/03602559.2012.663039
- [37] Aliyu IK, Samad MA, Al-Qutub A. Tribological characterization of a bearing coated with UHMWPE/GNPs nanocomposite coating. *Surf Eng.* 2021;37:60–69. doi:10.1080/02670844.2020.1754624
- [38] Tong J, Ma Y, Arnell RD, et al. Free abrasive wear behavior of UHMWPE composites filled with wollastonite fibers. *Compos Part A: Appl Sci Manuf.* 2006;37:38–45. doi:10.1016/j.compositesa.2005.05.023
- [39] Kanaga Karuppiyah KS, Bruck AL, Sundararajan S, et al. Friction and wear behavior of ultra-high molecular weight polyethylene as a function of polymer crystallinity. *Acta Biomater.* 2008;4:1401–1410. doi:10.1016/j.actbio.2008.02.022
- [40] Figueiredo-Pina CG, Dearnley PA. Influence of scratch damage to S phase coated and uncoated orthopaedic grade stainless steel on wear of ultrahigh molecular weight polyethylene. *Surf Eng.* 2012;28:683–692. doi:10.1179/1743294412Y.0000000022
- [41] Fan P, Xu W, Lu C, et al. Improving the compatibility of polycarbonate/UHMWPE blends through gamma-ray irradiation. *Int J Polym Anal Charact.* 2006;11:429–440. doi:10.1080/10236660601001304
- [42] Gratiela T, Daniela M, Gabriela R, et al. Effect of hydrophilic – hydrophobic balance on biocompatibility of poly (methyl methacrylate) (PMMA) – hydroxyapatite (HA) composites. *Mater Chem Phys.* 2009;118:265–269. doi:10.1016/j.matchemphys.2009.03.019